V International Conference on Particle-based Methods – Fundamentals and Applications
PARTICLES 2017
P. Wriggers, M. Bischoff, E. Oñate, D.R.J. Owen, & T. Zohdi (Eds)

THERMAL LATTICE BOLTZMANN SIMULATION OF DIFFUSION/ FORCED CONVECTION USING A DOUBLE MRT MODEL

BOGDAN KRAVETS, HARALD KRUGGEL-EMDEN

Mechanical Process Engineering and Solids Processing (MVTA)
Technical University Berlin (TU Berlin)
Ernst-Reuter-Platz 1, 10587 Berlin, Germany
e-mail: kravets@tu-berlin.de, kruggel-emden@tu-berlin.de, web page: http://www.mvta.tu-berlin.de

Key words: Particle, Heat Diffusion, Forced Convection, Thermal LBM, Double MRT approach.

Abstract. The Lattice-Boltzmann method (LBM) is an alternative and flexible approach for computational fluid dynamics (CFD). Unlike many other direct numerical simulation (DNS) techniques, LBM is not solving the Navier-Stokes equations but is based on the kinetic theory and the discrete Boltzmann equation. LBM utilizes a Cartesian mesh and hence does not require a complex mesh derivation or a re-meshing in case of moving boundaries. Thermal LBM (TLBM) which is capable of solving thermal convection/diffusion problems relies on a set of two distribution functions, the so called double distribution function (DDF) approach; one for the fluid density and one for the internal energy. For the carried out numerical investigations a 3D TLBM framework is derived involving a multiple-relaxation-time (MRT) collision operator for both, the fluid and the temperature field which is yet not applied widely. Hydrodynamic and thermal boundary conditions are represented by interpolated bounce back schemes. The derived TLBM framework is applied to diffusion and convection-diffusion problems (e.g. forced convection) for plane and curved boundaries and is validated against analytical solutions, when available or compared to established correlations. The thermal MRT operator is further compared against an existing LBM model based on a thermal Bhatnagar-Gross-Krook (BGK) operator regarding accuracy and numerical stability. Averaged and local heat transfer coefficients are presented. The findings indicate that the double MRT framework with interpolated boundary conditions offers a highly accurate and efficient approach for the analysis of heat transfer problems especially for particle/fluid systems under detailed resolved flow.

1 INTRODUCTION

CFD simulations of particle/fluid systems – like packed beds, fluidized beds and pneumatic conveying – which resolve the flow around particles, have become increasingly important in the past [1–8]. Resolved flow approaches provide the most detailed level of insight and can e.g. be applied for creating closure correlations for momentum [2–4] and heat transfer [5–8] for single particles and particle packings. Derived closures can be used for large particle/fluid systems where the flow conditions are prescribed by a non-resolved CFD approach as it is often the case in the DEM/CFD.

Established DNS methods rely mostly on solving the discretized Navier-Stokes equations

using particle surface-adapted meshes. A less frequently used technique to perform CFD simulations of particle/fluid systems is the so called lattice Boltzmann method (LBM). In contrast to other established DNS simulations, LBM relies on the discrete Boltzmann equation and is primary used in combination with an equidistant Cartesian grid. Thermal (LBM) relies on a double distribution function approach [9], where the hydrodynamic part is represented by density distributions f_i and the thermal part by energy distributions g_i. Here the hydrodynamic side can be prescribed by the Bhatnagar–Gross–Krook [10] or by multiple-relaxation-time collision models [11] and the thermal side was solely represented by the Bhatnagar–Gross–Krook model in the past [9]. MRT/MRT or double MRT models, meaning hydrodynamic and thermal part are solved by a MRT operator, were introduced most recently [12,13]. It should be noted, that the MRT collision operator is more advanced and is reported to be more accurate and stable than the BGK operator.

Boundary conditions have also a great influence on the simulations results regarding accuracy and stability. The most common boundary condition is the so called half way bounce back rule. Based on that very native method interpolated bounce back routines were presented for hydrodynamic [14] and thermal side [1]. Besides interpolated bounce back methods boundary conditions using energy balancing of a node under the usage of summation and target/actual-value comparison were introduced by Liu et al. [15]. The present study deals with the evaluation of the thermal MRT collision operators and the influence of thermal boundary conditions. A double MRT framework is compared against a MRT/BGK model using different boundary conditions with regard to numerical accuracy. Local and global heat transfer is addressed and compared to analytical solutions or to results obtained from scientific literature.

2 NUMERICAL METHOD

2.1 Lattice Boltzmann Method

The underlying numerical method of this investigation is a three dimensional double distribution function Lattice Boltzmann model. The fluid flow is represented by a multiple-relaxation-time collision operator (MRT) with 19 discrete velocity directions (D3Q19) as proposed by d'Humiéres et al. [11] which is described by the following expression:

$$f_i(\vec{x} + \vec{e_i}\Delta t, t + \Delta t) = f_i(\vec{x}, t) - \langle M^{-1} \cdot \hat{S} \cdot [m_i(\vec{x}, t) - {m_i}^{eq}(\vec{x}, t)]\rangle_i + F_i, \quad (1)$$

where f_i is the density distribution function, with $\vec{e}_i$ being the discrete velocity of each distribution function. In eq. (1) F_i is an external force which can be applied along the $i - th$ lattice direction if desired. M is a $n \times n$ transformation matrix and $\hat{S}$ a $n \times n$ diagonal collision matrix, with n being the number of discrete directions e.g. $n = 19$ for D3Q19. For a detailed description e.g. of the choice of relaxation rates or equilibrium momenta ${m_i}^{eq}$ the reader is referred to [11].

For the thermal side three collision operators are investigated here: a D3Q19 Bhatnagar-Gross-Krook operator (BGK) proposed by Peng et al. [16], which is given by:

$$g_i(\vec{x} + \vec{e}_i\Delta t, t + \Delta t) = g_i(\vec{x}, t) - \frac{1}{\tau_g}[g_i(\vec{x}, t) - {g_i}^{eq}(\vec{x}, t)], \quad (2)$$

a D3Q7 MRT and a D3Q19 MRT model proposed by Li et al. [12] which are based on the

model proposed by Yoshida and Nagaoka [13] and are represented by the following expression:

$$g_i(\vec{x} + \vec{e_i}\Delta t, t + \Delta t) = g_i(\vec{x}, t) - \langle M^{-1} \cdot \hat{S}_g \cdot \left[m_{i_g}(\vec{x}, t) - m_{i_g}^{eq}(\vec{x}, t) \right] \rangle_i . \quad (3)$$

In eqs. (2) and (3) g_i is the energy distribution function and M and $\hat{S}_g$ are transformation and collision matrix respectively. M is given in [11] for a D3Q19 and in [13] for a D3Q7 model. Li et al. [12] propose equilibrium momenta m^{eq} for both D3Q7 and D3Q19 schemes. The underlying discrete velocities for the D3Q7 and the D3Q19 model are shown in Figure 1.

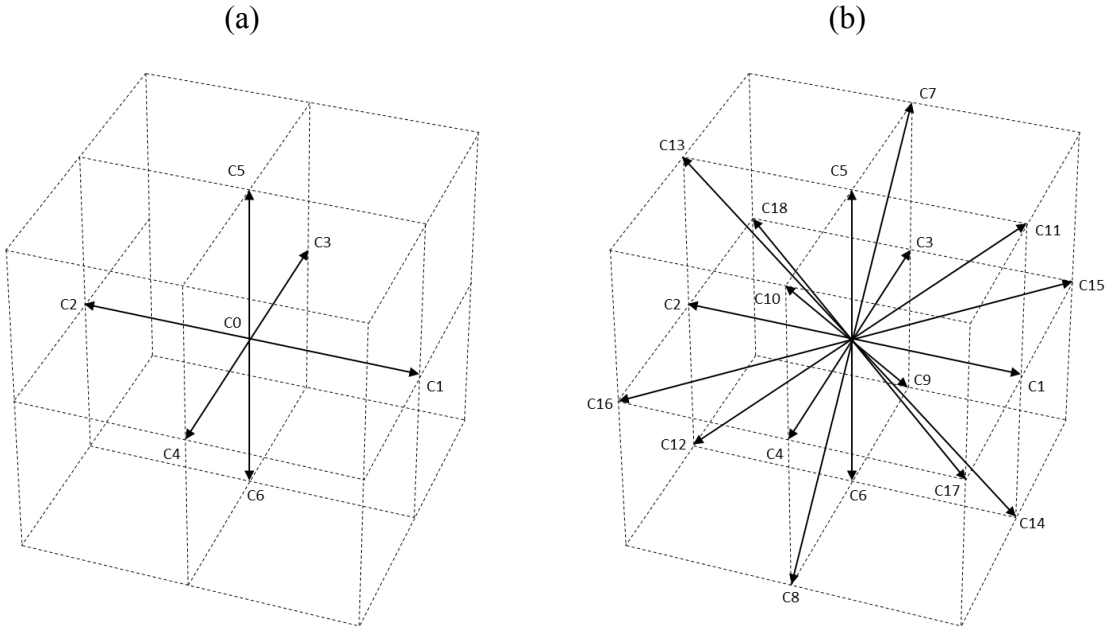

Figure 1: Discrete velocity vectors in (a) D3Q7 and (b) D3Q19 model.

2.2 Hydrodynamic Boundary Conditions

The most common hydrodynamic boundary condition in LBM is the so called bounce back rule, where the distribution function pointing outside the numerical domain is reflected in the reversed direction:

$$f_{\bar{i}}(\vec{r}_i, t + \Delta t) = f_i^*(\vec{r}_i, t), \quad (5)$$

where $f_{\bar{i}}$ denotes the unknown incoming density distribution and f_i^* denotes the post collision distribution function which points outwards towards the fluid boundary. Here it is assumed that the wall is located in the middle between two lattice nodes. In case the wall is not located at $\Delta x/2$ the interpolated bounce back rule proposed by Bouzidi et al. [14] can provide more accurate results. The unknown distribution functions can be prescribed by linear or by quadratic interpolation. In the present study only quadratic interpolation is used for the hydrodynamic boundary conditions. Figure 2 schematically shows the interpolated bounce back routine with dependence on the wall position q. For further details see [14].

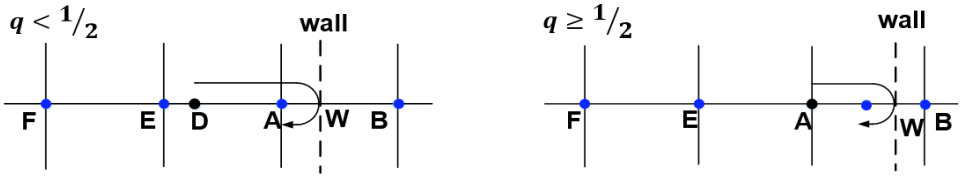

Figure 2: Schematic representation of the interpolated boundary condition [14].

2.3 Thermal Boundary Conditions

Based on the idea of the simple bounce back, Yoshida and Nagaoka [13] proposed the following thermal Dirichlet boundary condition:

$$g_{\bar{i}}(\vec{r}_i, t + \Delta t) = -g_i{}^*(\vec{r}_i, t) + \varepsilon_D \phi_D \tag{4}$$

Similar to the hydrodynamic boundary conditions $g_{\bar{i}}$ denotes the unknown energy distribution and $g_i{}^*$denotes the known post collision energy distribution which points outwards of the fluid domain towards the fluid boundary. With ϕ_D being the Dirichlet source term representing the internal energy at the regarded node and ε_D the Dirichlet coefficient which depends on the weighting factor of the LBM model [3,4]. Li et al. [1] extended this model to an interpolated thermal bounce back (similar to the hydrodynamic boundary condition proposed by Bouzidi et al. [14]) and proposed three different interpolation schemes of which scheme 1

$$g_{\bar{i}}(\vec{r}_i, t + \Delta t) = (-2q) g_i^*(\vec{r}_i, t) + (2q - 1) g_i^*(\vec{r}_i - \vec{e}_i, t) + \varepsilon_D \Phi_D \quad \text{for } q < \frac{1}{2}, \tag{5}$$

$$g_{\bar{i}}(\vec{r}_i, t + \Delta t) = -\frac{1}{2q} g_i^*(\vec{r}_i, t) + \frac{(2q - 1)}{2q} g_i^*(\vec{r}_i, t) + \frac{1}{2q} \varepsilon_D \Phi_D \quad \text{for } q \geq \frac{1}{2} \tag{6}$$

and scheme 3

$$g_{\bar{i}}(\vec{r_i}, t + \Delta t) = -\, g_i^*(\vec{r_i}, t) + \frac{(2q - 1)}{(2q + 1)} g_i^*(\vec{r_i} - \vec{e_i}, t) + \frac{(2q - 1)}{(2q + 1)} g_{\bar{i}}^*(\vec{r_i} - \vec{e_i}, t) + \frac{2\, \varepsilon_D \Phi_D}{(2q + 1)} \tag{7}$$

are considered in the present study. Scheme 1 and scheme 3 reduce to the simple thermal bounce back in eq. (4) for $q = 1/2$.

Apart from the interpolated thermal bounce back other thermal boundary conditions were proposed in the near past. Liu et al. [15] proposed the following thermal boundary rule:

$$g_{\bar{i}}(\vec{r}_i, t + \Delta t) = g_i{}^*(\vec{r}_i, t) + w_i G_c, \tag{8}$$

where $g_{\bar{i}}$ and $g_i{}^*$ are the unknown and known distributions respectively, w_i the weighting factor of the LBM model and G_c is the corrector which is enforcing the internal energy and is given as:

$$G_c = \frac{\rho_0 e - \rho_0 e^*}{\sum_{i=0}^{n} \omega_i}. \tag{9}$$

Here e^* is the target value for internal energy, and e is the actual internal energy and which can be determined by linear

$$\rho_0 e_A = \rho_0\big(e_W + (e_E - e_W)\big)\frac{\overline{AW}}{\overline{EW}}\,, \tag{10}$$

or by quadratic interpolation

$$\rho_0 e_A = \rho_0\left(e_W + (e_E - e_W)\frac{\overline{AW}}{\overline{EW}} + \Big(\frac{e_E - e_W}{\overline{EW}} - \frac{e_F - e_E}{\overline{EF}}\Big)\frac{\overline{AE}\cdot\overline{AW}}{\overline{FW}}\right). \tag{11}$$

The internal energy for a lattice can be obtained by the summation of all energy distributions $e = \sum_{i=0}^{n} g_i$. If the regarded point (e.g. E, F) doesn't coincide with the LBM mesh (curved boundary), trilinear interpolation is used to determine the value in this point. For details on the geometric properties / location of E, F see [17].

3 RESULTS

3.1 Heat diffusion cases

As an initial case a 1D diffusion problem is regarded. A simulation domain of the length L with constant boundary temperature $T_s = 10$ and the initial Temperature $T_{init} = 0$ was selected. To study the performance of the collision operators and boundary conditions the simulation domain was refined as follows: $L = 20, L = 40, L = 80, L = 160$ and $L = 320$. The boundary wall was located between two nodes (simple half way bounce back rule). Thermal MRT collision operators for D3Q7 and D3Q19 [13] as well as the thermal BGK operator for D3Q19 proposed by Peng et al. [16] were studied. Furthermore, two different boundary conditions [1,15] were investigated. Thermal relaxation time was set to $\tau_g = 0.53$ for all simulations. The obtained temperature profile was compared to an analytical solution.

This analytical solution for a 1D diffusion problem with constant boundary conditions is given by the following expression:

$$T(x,t) = T_s + (T_{init} - T_s)\sum_{n=0}^{\infty} a_n \exp\left(-\frac{n^2\pi^2\alpha t}{L^2}\right) sin\left(\frac{n\pi x}{L}\right), \tag{12}$$

where $a_n = 4/\pi n$ for odd n and zero for even n, α is the thermal conductivity and t the simulation time. The analytical expression can be used with physical or non-dimensional LBM quantities.

Figure 3 shows the averaged relative error for each simulation. As can be seen from the obtained results all investigated collision operators and boundary conditions are second order accurate in space. For 1D diffusion problems MRT D3Q7 provides the greatest accuracy which is in good agreement with results presented by Li et al. [1]. It can be noted, that the investigated thermal MRT models proposed by Yoshida and Nagaoka [13] are superior in terms of accuracy compared to thermal BGK proposed by Peng et al. [16]. Boundary conditions proposed by Yoshida and Nagaoka [13] are three to five times more accurate compared to boundary conditions proposed by Liu et al. [15]. It should be stressed out in conclusion, that the boundary conditions have a major influence on the numerical accuracy.

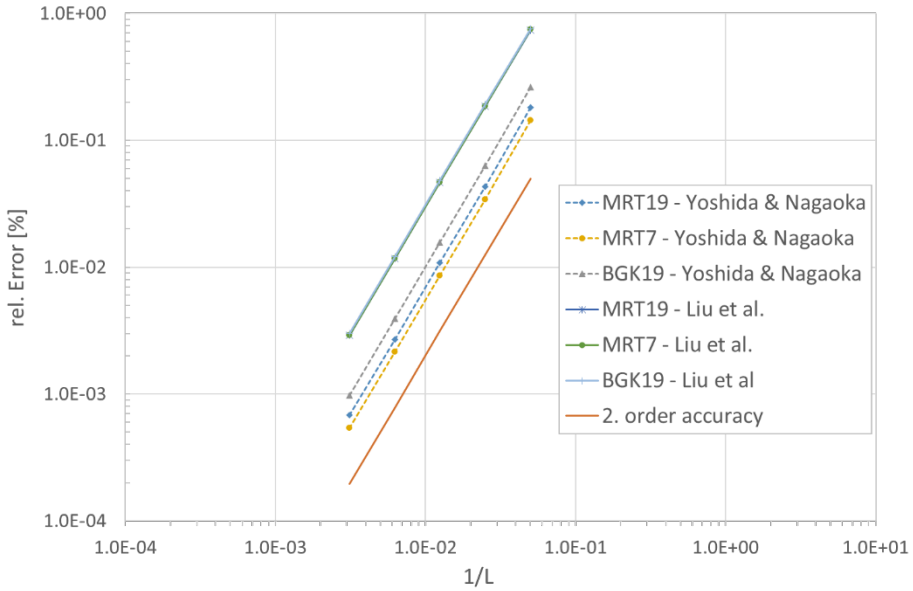

Figure 3: Relative error over grid resolution $1/L$ for the 1D thermal diffusion problem.

As second case a 3D diffusion problem is considered. The cubic domain of size $8 \cdot d_p$ has periodic boundaries. The particle diameter is varied as follows: $d_p = 5$, $d_p = 10$, $d_p = 20$ and $d_p = 40$. The thermal relaxation time was chosen as $\tau_g = 0.53$. The analytical solution to the described problem is given by

$$T(x,t) = T_s + (T_S - T_\infty)\frac{R}{x}\left(1 - erf\left(\frac{x-R}{\sqrt{4t\alpha}}\right)\right) \qquad for\ x > R, \tag{13}$$

where erf is the error function, x is the distance from the sphere center and R the particle radius. T_∞ is the temperature of the undisturbed fluid and can be considered as the initial temperature for a sufficient small simulation time t. Figure 4 shows the temperature distribution of the described case.

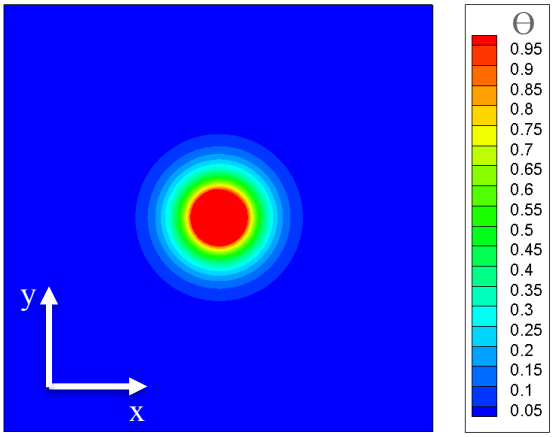

Figure 4: Distribution of dimensionless temperature $\theta = (T - T_i)/(T_s - T_i)$ around a fixed sphere.

In contrast to 1D diffusion problems – where the distance from wall to fluid node is constant for each node – curved boundaries have a different wall-node distance for every discrete node. This influences the numerical error as was shown by Li et al. [1]. It can be concluded from the presented results in Figure 5 that all investigated collision operators and boundary conditions provide second order accuracy for curved boundaries regarding the grid resolution. Thermal MRT collision operators [12,13] are more accurate compared to the investigated thermal BGK operator [16]. However, boundary conditions have a major influence on the numerical accuracy. It should be noted that boundary conditions proposed by Li et al. [1] have a greater numerical accuracy in the regarded case than the conditions proposed by Liu et al. [15].

In particular scheme 1 (eqs. (5)-(6)) provides the best accuracy. Linear and quadratic interpolated boundary conditions proposed by Liu et al. [15] rely on 3D interpolation routines to determine the exact node temperature which causes a greater numerical error and an irregular course. quadratic interpolated boundary conditions are superior to linear interpolated. Scheme 1 provides the greatest accuracy among all investigated boundary conditions.

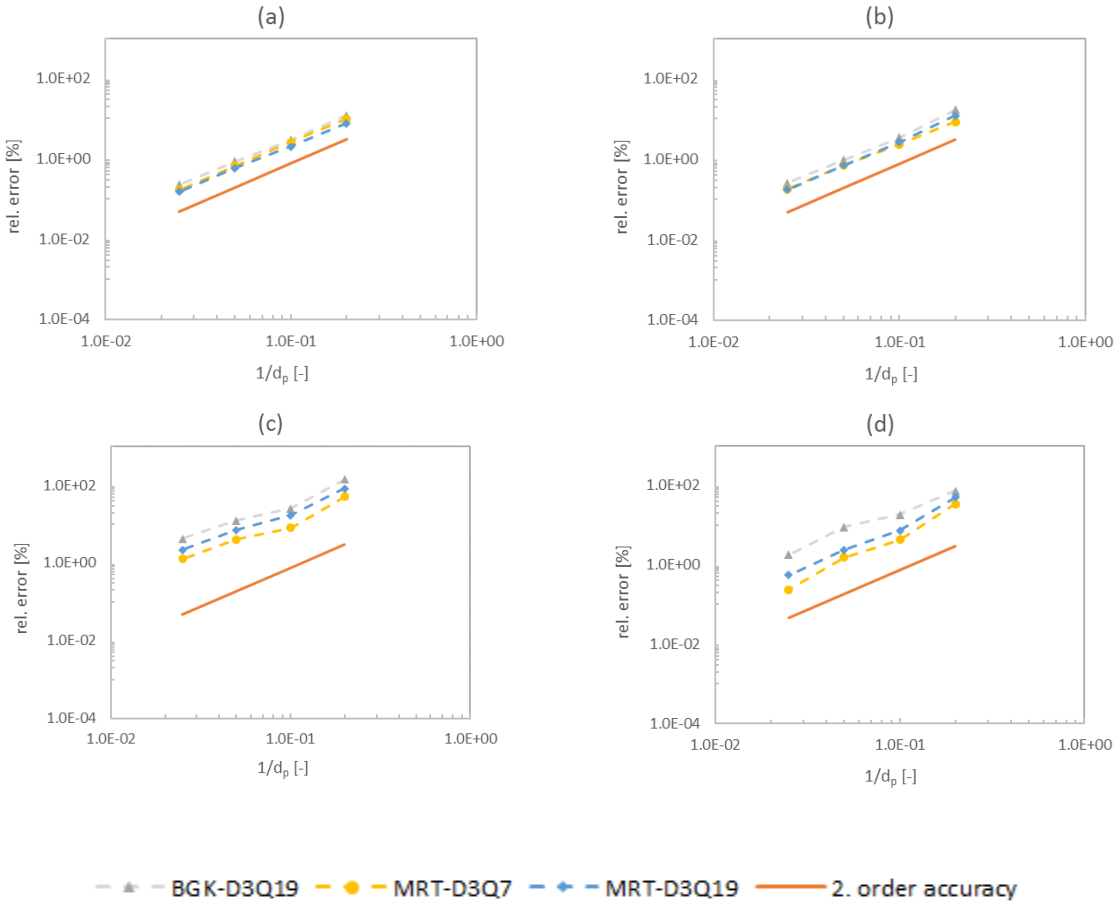

Figure 5: Relative error over grid resolution $1/d_p$ for diffusive heat transfer of an isothermal sphere: (a) thermal bounce back scheme 1, (b) thermal bounce back scheme 3, (c) linear interpolation and (d) quadratic interpolation.

3.2 Forced convection case

Numerical investigations of an isothermal sphere passed by a fluid were performed in order to study the influence of the convective part of the thermal LBM model. The Reynolds number was stepwise increase up to $Re = 800$ and the Prandtl number was set to $Pr = \nu/\alpha = 1$ for all simulations. To eliminate wall effects the simulation domain was chosen to be $30 \cdot d_p \times 15 \cdot d_p \times 15 \cdot d_p$ with $d_p = 40$ with adiabatic and free slip boundary conditions at walls parallel to the flow. The flow is initiated at $-x\ wall$ with a constant fluid velocity and temperature. To verify the correctness of the flow conditions and the accuracy of the implemented LBM framework the obtained drag coefficients C_D were compared against established scientific closure correlations [18–24] and experimental data [25]. Obtained drag coefficients are presented in Figure 6.

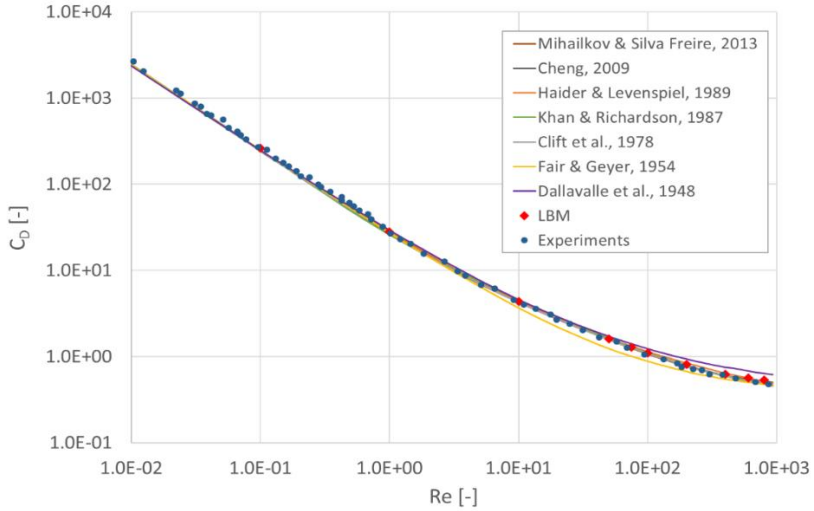

Figure 6: Drag coefficient over Reynolds number for a static sphere.

It can be concluded that the LBM reflects the flow conditions very accurately and in very good agreement with published results. If we regard the most recent correlation proposed by Mikhailov and Silva Freire [18] we obtain an average error of 3.72% for the present study.

For convection diffusion problems scheme 1 (eqs. (5)-(6)) proposed by Li et al. [1] with all introduced thermal collision operators were regarded. Particle averaged (or global) Nusselt numbers were evaluated and are presented in Figure 7 (a). Regarding the heat fluxes of the used set up, where the only heat sources are the domain inflow and the particle surface, and the heat sink is the domain outflow, the following relationship for the particle averaged Nusselt number can be derived:

$$Nu = \frac{U_0 A_{inlet}}{\pi d_p \alpha} \frac{(\bar{T}_{outlet} - \bar{T}_{inlet})}{(T_S - \bar{T}_{inlet})}, \tag{14}$$

where A_{inlet} is the surface area of the inlet, U_0 the fluid velocity (or superficial velocity) at the inlet, $\bar{T}_{outlet}$ and $\bar{T}_{inlet}$ are the velocity averaged fluid temperatures at the inlet and outlet of the domain and T_S is the particle surface temperature.

It can be concluded from the obtained results, that thermal BGK and MRT models prove high accurate results for convection-diffusion problems. However, the BGK operator remains stable only up to $Re = 240$ for $d_p = 40$. Thermal MRT models are up to three times more numerically stable than the thermal BGK model. Please note that the thermal BGK referred in this work is the collision operator proposed by Peng et al. [16]. It should be noted that BGK operators with a different g^{eq} may behave differently.

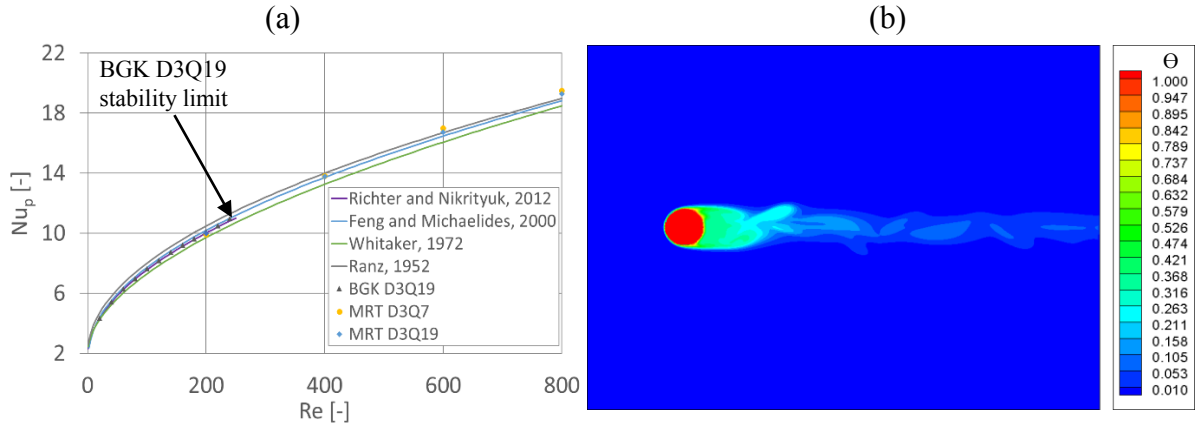

Figure 7: (a) Nusselt numbers over Reynolds numbers for a sphere attributed to forced convection at $Pr = 1$ (b) Distribution of dimensionless temperature $\theta = (T - T_{inlelt})/(T_s - T_{inlet})$ for $Re = 800$ and $Pr = 1$ prescribed with a double MRT D3Q19 model and scheme 1 (eq. (5)-(6)) at the sphere surface.

To evaluate local heat transfer coefficients, the temperature gradient at the boundaries is regarded:

$$Nu_i = h_f \cdot \frac{d_p}{k_f} = \frac{\partial T_i}{\partial x_i} \frac{d_p}{(T_S - T_{ref})}, \tag{15}$$

where Index i represents the $i-th$ boundary node in which the local Nusselt number is evaluated. The particle diameter d_p is the reference length, T_S is the particle surface temperature and T_{ref} is the particle reference temperature which is here the temperature of the undisturbed fluid ($\bar{T}_{inlet}$). Apart from eq. (14) particle averaged Nusselt numbers can also be obtained by surface integration:

$$Nu = \frac{1}{\pi d_p^2} \int Nu_i dA \tag{16}$$

If the treatment is discrete, we can simplify this equation to $\mathrm{Nu} = \sum Nu_i / n_{nodes}$. Nu_i is the local Nusselt number (see eq. (15)) and n_{nodes} the number of considered discrete nodes. For more details on calculation of local heat transfer coefficients see [26].

Figure 8 (a) shows the obtained Nusselt numbers plotted over the corresponding polar angle ϕ for $\mathrm{Re} = 200$ and $\mathrm{Pr} = 1$.The maximum of the Nusselt number is located at the front stagnation point ($\phi = 0°$) while the minimum can be found at $\phi \approx 130°$ for the presented Reynolds number. The obtained results are compared to numerical studies by Dhole et al. [27].

It can be concluded, that the thermal MRT and the BGK models in combination with scheme 1 provide not only very accurate particle averaged Nusselt numbers but also accurately reflect their local distribution. The deviations to Dhole et al. [27] can be explained by the advantage of surface adapted meshes used in the introduced study. Especially the evaluation in a Cartesian mesh is regarded as a limiting factor. As can be seen in Figure 8 (a) and (b) D3Q7 suffers from notable over- and underestimation in the area of the curved boundary ($\phi \approx 20 - 70°$). This can be explained by the lack of some of the discrete velocities in the D3Q7 model which are however provided in the D3Q19 model.

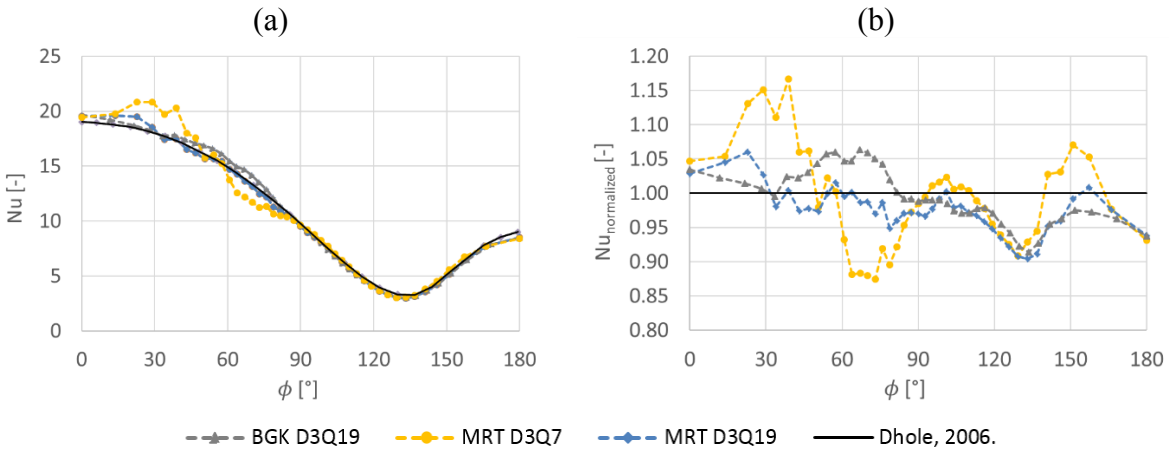

Figure 8: (a) Local Nusselt numbers of a sphere over polar angle ϕ for $Re = 200$ and $Pr = 1$ (b) Local Nusselt numbers normalized with results by Dhole et al. [27].

4 CONCLUSIONS

- A thermal LBM framework based on a double MRT model has been derived and its performance has been evaluated. Diffusion and convection-diffusion problems for plane and curved boundaries have been studied. It was shown that the presented LBM models provide highly accurate results for particle averaged and local heat transfer coefficients. Second order accuracy in space for all cases was achieved.
- MRT/MRT models [12] are superior to MRT/BGK [16] models in terms of numerical stability and accuracy. Double MRT models are up to three times more stable than the investigated thermal BGK operator.
- For curved boundaries the D3Q19 model provides more accurate results than the D3Q7 model, especially when the local heat transfer distribution is regarded. D3Q7 suffers from notable over- and underestimation in the area of the curved boundary ($\phi \approx 20 - 70°$) due to possibly the lack of some discrete velocities in the D3Q7 model.
- Thermal boundary conditions based on the thermal bounce back idea [1], are more accurate compared to boundary conditions based on energy balance and the usage of target/actual-value comparison [15]. Furthermore, methods based on the bounce back idea are far more efficient, since no 3D interpolation is required.

REFERENCES

[1] Li, L., Mei, R. and Klausner, J.F. Boundary conditions for thermal lattice Boltzmann equation method. *J. Comput. Phys.* (2013) **237**:366–395.

[2] Hill, R.J., Koch, D.L. and Ladd, A.J.C. The first effects of fluid inertia on flows in ordered and random arrays of spheres. *J. Fluid Mech.* (2001) **448**:213–241.

[3] Hill, R.J., Koch, D.L. and Ladd, A.J.C. Moderate-Reynolds-number flows in ordered and random arrays of spheres. *J. Fluid Mech.* (2001) **448**:243–278.

[4] Beetstra, R., Van Der Hoef, M.A. and Kuipers, J.A.M. Drag force of intermediate reynolds number flow past mono- and bidisperse arrays of spheres. *AIChE J.* (2007) **53**:489–501.

[5] Gunn, D.J. Transfer of heat or mass to particles in fixed and fluidised beds. *Int. J. Heat Mass Transf.* (1978) **21**:467–476.

[6] Gnielinski, V. Wärme- und Stoffübertragung in Festbetten. *Chemie Ing. Tech.* (1980) **52**:228–236.

[7] Tavassoli, H., Peters, E.A.J.F. and Kuipers, J.A.M. Direct numerical simulation of fluid-particle heat transfer in fixed random arrays of non-spherical particles. *Chem. Eng. Sci.* (2015) **129**:42–48.

[8] Wakao, N., Kaguei, S. and Funazkri, T. Effect of fluid dispersion coefficients on particle-to-fluid heat transfer coefficients in packed beds. Correlation of nusselt numbers, *Chem. Eng. Sci.* (1979) **34**:325–336.

[9] He, X., Chen, S. and Doolen, G.D. A Novel Thermal Model for the Lattice Boltzmann Method in Incompressible Limit. *J. Comput. Phys.* (1998) **146**:282–300.

[10] Bhatnagar, P.L., Gross, E.P. and Krook, M. A Model for Collision Processes in Gases. I. Small Amplitude Processes in Charged and Neutral One-Component Systems. *Phys. Rev.* (1954) **94**:511–525.

[11] D'Humières, D., Ginzburg, I., Krafczyk, M., Lallemand, P. and Luo, L.-S. Multiple-relaxation-time lattice Boltzmann models in three dimensions. *Philos. Trans. A. Math. Phys. Eng. Sci.* (2002) **360**:437–451.

[12] Li, L., Mei, R. and Klausner, J.F. Lattice Boltzmann models for the convection-diffusion equation: D2Q5 vs D2Q9. *Int. J. Heat Mass Transf.* (2017) **108**:41–62.

[13] Yoshida, H. and Nagaoka, M. Multiple-relaxation-time lattice Boltzmann model for the convection and anisotropic diffusion equation. *J. Comput. Phys.* (2010) **2297**:774–7795.

[14] Bouzidi, M., Firdaouss, M. and Lallemand, P. Momentum transfer of a Boltzmann-lattice fluid with boundaries, *Phys. Fluids.* (2001) 13:3452–3459.

[15] Liu, C.-H., Lin, K.-H., Mai, H.-C. and Lin, C.-A. Thermal boundary conditions for thermal lattice Boltzmann simulations, *Comput. Math. with Appl.* (2010) **59**:2178–2193.

[16] Peng, Y., Shu, C. and Chew, Y.T. Simplified thermal lattice Boltzmann model for incompressible thermal flows, *Phys. Rev. E.* (2003) **68**:26701.

[17] Kruggel-Emden, H., Kravets, B., Suryanarayana, M.K. and Jasevicius, R. Direct numerical simulation of coupled fluid flow and heat transfer for single particles and particle packings by a LBM-approach. *Powder Technol.* (2016) **294**:236–251.

[18] Mikhailov, M.D. and Freire, A.P.S. The drag coefficient of a sphere: An approximation using Shanks transform. *Powder Technol.* (2013) **237**:432–435.
[19] Cheng, N.S., Comparison of formulas for drag coefficient and settling velocity of spherical particles. Powder Technol. (2009) **189**:395–398.
[20] Haider, A. and Levenspiel, O. Drag coefficient and terminal velocity of spherical and nonspherical particles. *Powder Technol.* (1989) **58**:63–70.
[21] Khan, A.R. and Richardson, J.F. The Resistance To Motion of a Solid Sphere in a Fluid, Chem. Eng. Commun. (1987) **62**:135–150.
[22] Clift, M.E., Grace, R. and Weber, J.R. Bubbles, Drops and Particles. (1978).
[23] Fair, G.M. and Geyer, J.C. Water Supply and Waste-water Disposal, Wiley, (1954).
[24] DallaValle, J.M. and Klemin, A., Micromeritics: the technology of fine particles. (1943) 428 .
[25] Schlichting, H. and Gersten, K. Boundary-Layer Theory, Vol. IX (2017).
[26] Kravets, B. and Kruggel-Emden, H. Investigation of local heat transfer in random particle packings by a fully resolved LBM-approach. *Powder Technol.* (2017) **318**:293–305.
[27] Dhole, S.D., Chhabra, R.P. and Eswaran, V. A numerical study on the forced convection heat transfer from an isothermal and isoflux sphere in the steady symmetric flow regime. *Int. J. Heat Mass Transf.* (2006) **49**:984–994.